Tip-Sample Capacitance in STM(STM-BEEM interfaces)

Sci. Rep. RITU A44 (1997) pp. 173-179
No. 2, March 1997

Tip-Sample Capacitance in STM

Shu Kurokawa and Akira Sakai
Mesoscopic Materials Research Center, Faculty of Engineering, Kyoto University, Sakyo-ku, Kyoto 606-01 Japan

(Received January 21, 1997)

We report in this paper the current status of theoretical and experimental researches on the STM capacitance. We find some essential inconsistencies among previous work, particularly in the gap dependence of the STM capacitance. We also present the results of our recent experiments which suggest a classical behavior of the STM capacitance at least just before the onset of tunneling.

KEYWORDS: STM, capacitance, mesoscopic capacitor, tunneling, Coulomb blockade

1. Introduction

STM (scanning tunneling microscopy) can be regarded as a capacitor with vacuum gap as an insulating layer between tip and sample. At large separations, this STM capacitor is expected to behave as an ordinary capacitor and its characteristics should be described by classical electrostatics. It is however not trivial that the classical behavior continues to be observed at smaller distances. Consider, for example, the gap dependence of the STM capacitance. A simple approximation of STM as a parallel plate capacitor gives a familiar $1/s$ dependence of the capacitance on the gap distance s. This capacitance diverges to infinity as s reduces to zero. More realistic approximation of the tip-sample geometry leads to various complicated capacitance formulae, but all of them predict singular behavior at $s = 0$. Since there should be no singularity in nature, something should happen as we reduce the gap distance; there might be some quantum effects in capacitance which remove the divergence at $s = 0$, or a new physical interpretation of capacitance might be necessary at smaller distances. No definite answer to this fundamental problem has been obtained so far.

STM is just suited to study this capacitance problem. The most important advantage of STM over other capacitors is its capability of varying the tip-sample separation from large values down to atomistic proximity. Although a variety of nano-sized capacitors have been fabricated, none of them have comparable control over the gap distance.

In this report, we will present a review of theoretical and experimental work on the STM capacitance. Starting with the description of some theoretical approaches in §2, we will make a brief survey of previous experiments directly or indirectly related to the STM capacitance in §3 and point out some unsolved basic problems in §4. Experimental results of our own research on the STM capacitance, which has not been complete yet, will be presented and discussed in §5.

2. Theoretical Implications on the STM Capacitance

There have been an increasing number of theoretical researches on ultrasmall capacitors with the development of the nano-electronics. The main target of these researches however resides in the capacitive properties of nanostructures, like quantum dots in particular. No theoretical work has been made so far on the STM capacitance. Nevertheless some theoretical results obtained on ultrasmall capacitors are also applied to STM and of some interest here.

Microscopic effects in small capacitors have been first discussed by Lang and Kohn [1] in their treatment of the response of metal surfaces to an external electric field. They pointed out that the effective gap distance for capacitive effects between two parallel electrodes is slightly larger than the tunneling distance concerned with electron tunneling phenomena. The difference in two distances is typically 0.1 nm. It thus makes no effects in macroscopic capacitors but becomes non-negligible in small-gap capacitors.

Büttiker and his coworkers have recently carried out intensive theoretical analyses of nanostructured "mesoscopic" capacitors. [2-5] An important result of their analyses is the distinction between geometrical and electrochemical capacitances. The former is a usual classical capacitance determined by electrode geometry, $C_0 = dQ/dU$ where Q and U are a charge on an electrode and an applied voltage drop, respectively. The latter is on the other hand related to electron transfer between two electrodes and formally defined as $C_\mu = edQ/d\mu$ where μ is a chemical potential of electrons. For mesoscopic capacitors, C_μ is no longer equal to C_0. Their difference arises from the fact that the macroscopic voltage drop applied to a mesoscopic capacitor can differ significantly from the microscopic drop of the electrostatic potential between electrode surfaces. Büttiker [3] has shown that this difference can be written in terms of the electron screening length λ and obtained the following expres-

sion for parallel plate capacitors,

$$C_\mu = 1/(C_0^{-1} + 2\lambda/\epsilon_0 A) \quad (1)$$

where A is an electrode area. Equation 1 thus has a simple interpretation that the field penetration into each electrode effectively expand the electrode separation. It is interesting that the capacitance of eq. (1) does not diverge and takes a finite value even when the geometrical capacitance C_0 goes to infinity ($C_0^{-1} \to 0$).

The electrochemical capacitance is relevant to electron transfer and can therefore be identified as a tunneling capacitance which determines the capacitive phenomena associated with electron tunneling. Extension of eq. (1) to mesoscopic tunneling junctions has been recently carried out by Christen and Büttiker [4] who obtained a following simple formula for a single-channel point contact,

$$C_\mu = R/(C_0^{-1} + 2\lambda/\epsilon_0 A) \quad (2)$$

where R is the reflection probability of the channel. Note that C_μ vanishes for $s \to 0$ ($R \to 0$) even when C_0 diverges. Since R varies as $1 - e^{-\kappa s}$ in STM junctions, C_μ also has an exponential gap dependence for small separations (large C_0).

Another "tunneling capacitance", which might be physically different from the electrochemical capacitance, can be introduced when one considers the tunneling of individual electrons. Electron tunneling is a dynamical process taking place within a time scale given by $\tau = s/v_F$ where v_F is the Fermi velocity of electrons. The electromagnetic perturbation generated by one electron tunneling propagates through the electrodes to the distance $d = \tau c = s(c/v_F)$ where c is the speed of light. Therefore only the part of electrode within this distance can respond to the electron tunneling and contribute to the capacitance. In other words, a tunneling electron sees only small area of the electrodes. Other areas far from the tunneling point have no effects on tunneling. As a result, the tunneling capacitance becomes much smaller than the geometrical capacitance where all parts of electrode make some contribution according to classical electrostatics. If we take $s = 1$ nm for example, this tunneling capacitance is estimated to be ~ 1.3 fF.

This dynamic consideration of the tunneling capacitance is often applied to the charging effects (Coulomb blockade) of small tunneling junctions and known as the "horizon model". However nothing has been understood for its relation to the electrochemical capacitance of eq. (2) nor its applicability to STM junctions. We therefore will not further discuss this dynamic tunneling capacitance in following sections.

The distinction of geometrical and electrochemical or tunneling capacitance leads to a "two-capacitance model" that a small-gap tunneling junction has two physically different capacitances at the same time. Depending on the nature of experiments, one obtains either the geometrical capacitance or the electrochemical capacitance. Specifically, the capacitance measured in electron tunneling experiments must be the electrochemical (or tunneling) capacitance. In the next section, we review previous experiments on STM capacitance and in §4, we point out some inconsistencies in the data of STM capacitance and discuss them from the point of view of this "two-capacitance model".

3. Experimental Information on the STM Capacitance

3.1. Scanning capacitance microscopy

Tip-sample capacitance is of direct concern in scanning capacitance microscopy (SCaM). [6–11] In topographic SCaM experiments, a surface profile can be imaged through the sensitivity of tip-sample capacitance to the gap distance. A probe tip is scanned over a sample at constant height, and a small variation of capacitance is monitored with the RCA-type capacitance-detection system. [6] Therefore the gap sensitivity of capacitance dC/ds at some fixed tip position, not the whole $C - s$ behavior, is of practical importance in SCaM.

For needle-like tips, the tip-sample capacitance is usually approximated by a capacitance between a sphere (radius R) and an infinite plane. The sphere-plane capacitance is obtained only in a form of series expansion. For $s \ll R$, however, it can be written as

$$C = 4\pi\epsilon_0 R[1 - (1/2)\ln(s/8R)] \quad (3)$$

The capacitance therefore diverges logarithmically with s. This $\ln s$ dependence of the capacitance predicted in eq. (3) has been experimentally observed down to 100 nm by Akama *et al.* [9] From eq. (3), we also obtain for $s \ll R$

$$dC/ds = -2\pi\epsilon_0 R/s \quad (4)$$

The transition of the sensitivity dC/ds from $(R/s)^2$ to R/s in the proximity region has been pointed out by Kleinknecht *et al.* [10] However, with the development of AFM (atomic force microscopy), topographic SCaM experiments have been entirely replaced by AFM imaging, and no further measuremnets of $C - s$ nor $dC/ds - s$ characteristics have been performed with SCaM.

3.2. Electrostatic force microscopy

In electrostatic force microscopy, [12–14] one applies an ac voltage V to the AFM tip and measures the capacitive force F between tip and sample of the form

$$F = -(V^2/2)dC/ds \quad (5)$$

This force is therefore directly proportional to dC/ds. Application of electrostatic force microscopy is, however, aimed not at the measurement of the tip-sample capacitance itself but the monitoring of subsurface dopant profiles in semiconductors. Therefore only a few experimental data are available on dC/ds and its gap dependence.

Martin *et al.* [12] carried out the force measurements down to a few nm and find that the parallel-plate capacitor model (*i.e.* $dC/ds \propto 1/s^2$) gives a good agreement with experiment. On the other hand, Yokoyama *et al.* [14] report weak s dependence of dC/ds. Their data can be fitted to $\ln s$ rather than $1/s^2$. Based on

the scaling arguments, they also verify that the dC/ds of conical tips shows the observed $\ln s$ dependence. If dC/ds is proportional to $\ln s$, integration of dC/ds gives following expression for C,

$$C = A + Bs[1 + \ln(h/s)] \quad (6)$$

where A, B, h are constants. This formula apparently resembles with eq. (3) but has quite a different characteristics. As $s \to 0$, eq. (3) diverges logarithmically whereas eq. (6) gives a finite capacitance and changes almost linearly with s. This anomalous behavior is also incompatible with the $1/s$ dependence of C observed by Martin *et al.* [12] Experiments of electrostatic force microscopy therefore show no substantial agreement on the form of $C - s$ characteristics.

3.3. Coulomb blockade

Coulomb blockade in small tunneling junctions provides us a direct and quantitative estimation of junction capacitance. In Coulomb blockade experiments, the junction capacitance is calculated from the Coulomb gap $2e/C$ which can be obtained either from the period of the Coulomb staircase or from the asymptotic behavior of the $I - V$ curve.

A number of Coulomb blockade experiments in STM junctions have been reported so far. [15–21] The estimation of the STM capacitance is not, however, straightforward since a single tunneling junction like STM is well known to manifest only incomplete Coulomb blockade because of the charge fluctuation on the electrodes coupled to the "environment". Most experiments are therefore carried out on double junctions with small particles, clusters, and molecular aggregates as an intermediate electrode. The tunneling capacitor is formed between the tip and the intermediate electrode, and its capacitance is determined from from the Coulomb gap. The gap dependence can be obtained by plotting the capacitance as a function of tunneling current or conductance. In spite of a variety of materials used for the intermediate electrode, all Coulomb blockade experiments agree as to the gap dependence of the tip-electrode capacitance and consistently give the $1/s$ behavior of the capacitance. It should be noted that the magnitude of the capacitance at tunneling distances is found to be quite small, $1 \sim 5$ aF (1 aF $= 10^{-18}$ F).

3.4. Ultrafast STM

Quite different way of obtaining the STM capacitance is to measure the time constant $\tau = RC$ of STM junction, where R is the junction (tunneling) resistance. As τ is much smaller than the usual time scale of STM experiments, a special fast detection system is needed for such a measurement. Weiss *et al.* [22] incorporated photoexcited switches into STM and developed an ultrafast STM. These photoswitches are operated by laser pulses and used to generate and time-gate the tunneling current. By using subpicosecond pulsed lasers, they have succeeded to measure the transient response of the tunneling gap. Their analysis shows that the STM capacitance ranges $10^{-19} \sim 10^{-21}$ F and varies in proportion to the tunneling conductance, *i.e.* $C \propto e^{-\kappa s}$. Based on these results, they conclude that the STM capacitance is essentially different from the classical geometrical capacitance and is thus of quantum mechanical origin.

Groeneveld and van Kampen [23] have recently carried out similar ultrafast STM experiment but obtained a different conclusion. Their new analysis shows that the transient signal picked up by the STM tip is entirely due to the tip-sample coupling through the geometrical capacitance. If their interpretation is correct, the nonclassical tunneling capacitance would not be necessary for explaining the results of ultrafast STM. Again the experimental information on the STM capacitance is inconclusive.

4. Problems of the STM Capacitance

Some basic problems of the STM capacitance emerge from the above survey of previous experiments. First there is a huge diversity in capacitance values. If we take the results of Weiss *et al.* [22], the ultrafast STM gives a capacitance of the order of $10^{-19} \sim 10^{-21}$ F whereas the SCaM capacitance extrapolated to the tunneling region becomes $10^{-14} \sim 10^{-16}$ F.

Such a large numerical discrepancy can be reconciled if we adopt the "two capacitance model" discussed in §2. According to this model, a small junction shows two different capacitances depending on the method of experiment. Since electron tunneling is involved in ultrafast STM but not in SCaM and electrostatic force microscopy, a natural assignment is that former experiment give the electrochemical (tunneling) capacitance while the latter two measure the geometrical capacitance. Then the discrepancy among capacitance data no longer becomes a serious problem because these two capacitances can differ much in magnitude.

This interpretation based on the "two capacitance model" however brings about the second problem, that is the gap dependence of the STM capacitance. For geometrical capacitance, SCaM and force microscopy predict different gap dependence. The SCaM capacitance varies with $\ln s$ for small separations (eq. (3)) whereas the electrostatic force microscopy gives either $1/s$ or eq. (6) depending on experiments. The $C - s$ characteristics of the tunneling capacitance is more controversial. The exponential dependence $C \propto e^{-\kappa s}$ derived from the ultrafast STM is not observed in the Coulomb blockade experiments which support the $1/s$ behavior. Neither of these functional forms is consistent with that of the theoretical electrochemical capacitance given in eq. (2) which predicts a vanishing capacitance at $s = 0$.

The "two capacitance model" also meets some difficulty when explaining the results of Coulomb blockade experiments. Since Coulomb blockade is related to electron tunneling, the capacitance obtained from the Coulomb blockade experiments should be interpreted as electrochemical or tunneling capacitance. The magnitude of the capacitance, $\sim 10^{-18}$ F, which is again much smaller than the SCaM data, appears to support this interpretation. However this small capacitance can be accounted by the nano-scale size of particles or islands used

as the intermediate electrode. Substituting the size of these electrodes into the classical formula for a parallel-plate capacitor, one usually obtains a good estimation of the capacitance data. One therefore cannot determine on experimental basis whether the tip-electrode capacitance of double junctions is geometrical or electrochemical. This ambiguity will be removed if we carry out Coulomb blockade experiments on *single* STM junctions. Unfortunately single tunnel junctions show only minor charging effects, and no reliable data of $2e/C$ has been obtained at present on single STM junctions.

Kauppinen and Pekola [24] have recently pointed out that even in single junctions, the charging effects appear as a zero bias anomaly (ZBA), *i.e.* a conductance drop at zero bias. The junction capacitance can be obtained from the depth of the conductance dip. Although no such ZBA has been reported so far on STM junctions, its existence cannot be ruled out since the ZBA is likely to be confused with artifacts. Systematic search of ZBA in STM junctions (at low temperatures) will thus be of much value for elucidating the STM capacitance.

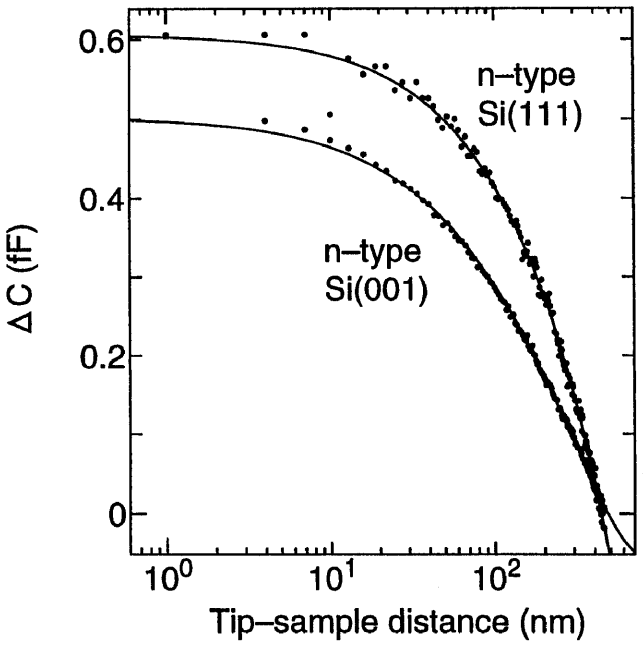

Figure 1. Gap dependence of the tip-sample capacitance measured on Si(001)2×1 and Si(111)7×7 surfaces. Solid curves represent the data fit to eq. (6).

5. Direct Measurements of the Gap Dependence of Tip-Sample Capacitance

5.1. Non-tunneling region

Discussion from §2 through §4 clearly indicates the lack of unified understanding on the nature of tip-sample capacitance in STM. In order to establish an experimental firm basis for further studies, we are undertaking direct measurements of the gap dependence of the tip-sample capacitance. We have started our experiment from the classical, non-tunneling region and expected to extend it into the tunneling region. Measurements in the non-tunneling region have been almost completed and some of their main results are presented here in a heuristic way.

We measure the tip-sample capacitance C directly using an AC capacitance bridge with a sensitivity of ~ 2 aF (Andeen-Hagerling 2500A). Because of a large stray capacitance (~ 0.5 pF), such a measurement does not give accurate values of C which is the order of fF. Nevertheless we can detect a relative change of C with varying the gap distance s provided that the stray capacitance stays constant with s. As the stray capacitance is of macroscopic origin, we can safely assume that the change in s of less than 1 μm should cause no significant changes in the stray capacitance and the observed change in the capacitance should be attributed to that of tip-sample capacitance. We have carried out some capacitance measurements without a tip and confirmed that the variation of the stray capacitance is actually negligible.

Surface contaminations, particularly polar water molecules, are known to give large unwanted contribution to the capacitance. We therefore started with clean silicon surfaces because of their ease in surface cleaning. [25] Typical $C-s$ curves obtained on Si(001) 2×1 and Si(111) 7×7 are shown in Fig. 1. The capacitance data at $s=600$ nm is arbitrary chosen as a reference and the change from that reference value is plotted against $\ln s$. We use a logarithmic distance scale to find any deviations from eq. (3), which characterizes the SCaM capacitance for $s>100$ nm. Both good agreement with eq. (3) for $s>100$ nm and a marked deviation at smaller separations are evident in the figure.

We first examined whether the apparent deviation from eq. (3) has some relation to the space charge layer of these semiconductor surfaces. [26] Experiments on p- and n-type substrates and the $C-V$ measurements on Si(001) and Si(111) revealed that the space charge layer has no effects on the observed $\Delta C-s$ curves.

Next we happened to find that the capacitance given by eq. (6) behaves quite similarly with the observed capacitance shown in Fig. 1. We therefore tried to fit the $C-s$ data by eq. (6) and obtained solid lines in Fig. 1. Agreement with the data is excellent over the entire range of s. This result is quite indicative of a conical tip geometry assumed in eq. (6). However the conical tip model is found to have some difficulties. First there is no way of relating the parameters in eq. (6) to the tip geometry. Since Yokoyama *et al.* [14] derived the linear relation between dC/ds and $\ln s$ purely from the geometrical scaling, they did not give any physical meaning to the parameters. Approximating a conical tip by a truncated polygonal pyramid, we could express these parameters in terms of height and cone angle of a tip but failed to obtain physically reasonable tip shapes from the fitting to the experimental data. Second it is quite hard to imagine that a real tip apex at a distance less than 100 nm still can be treated as a conical singularity.

In order to shed more light on the problem of tip shape, we made SEM observations of tip apex and tried to find some empirical relation between the tip radius

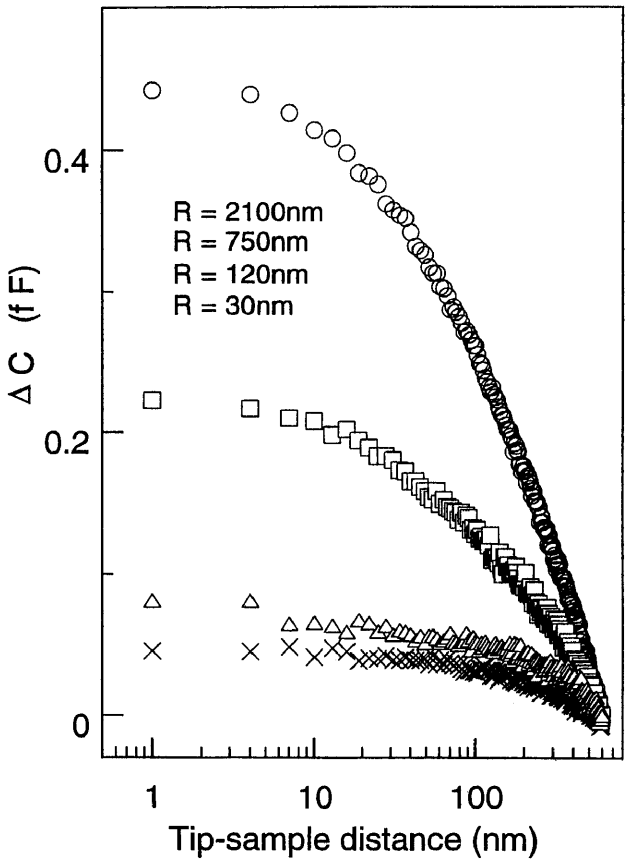

Figure 2. Gap dependence of the tip-sample capacitance obtained on tips of different radius R. The sample surface is Au(111).

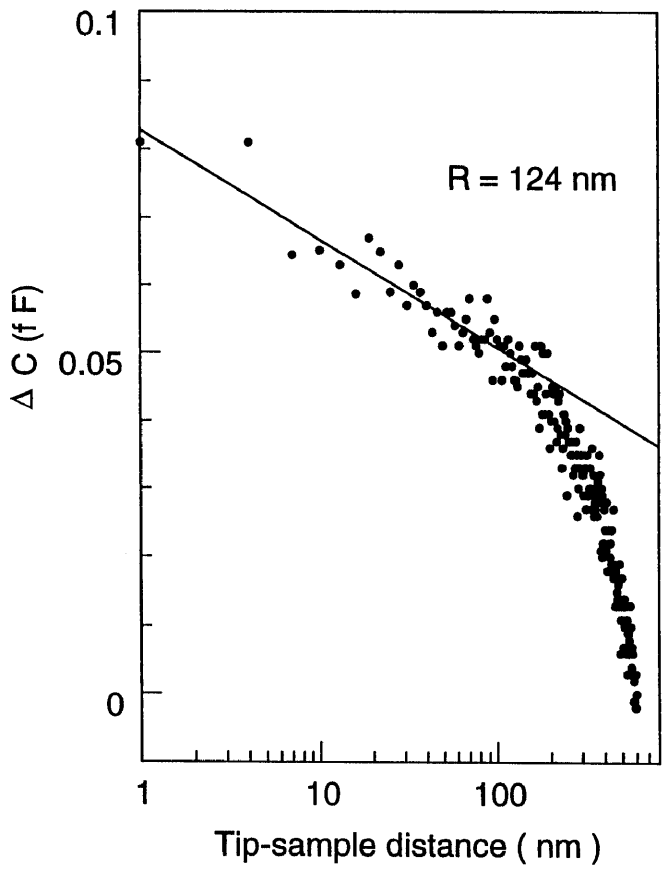

Figure 3. Enlarged plot of the $\Delta C - s$ curve for a 120 nm tip shown in Fig. 2. A solid line is the data fit to eq. (3). Only the part of the $\Delta C - s$ curve satisfying $s < R$ is used for fitting. Tip radius calculated from the slope by using eq. (4) is also shown in the figure.

and the capacitance characteristics. This new series of capacitance measurements has been made on clean Au(111) surfaces. As shown in Fig. 2, the observed ΔC curves are more or less the same as before. The slope of the $\Delta C - \ln s$ curve is much reduced for $s < 100$ nm. However, the magnitude of ΔC shows clear correlation with the tip radius; sharp tips produce smaller changes in ΔC than dull tips. A large variation of the magnitude of ΔC has been noticed before in experiments on Si surfaces [25] and speculated to be a tip effect, but its origin had not been clarified. Figure 2 clearly indicates that the magnitude of ΔC depends on the tip radius.

Another important consequence of SEM observations is that for sharp tips, the tip radius is smaller than the maximum gap distance of our measurements. The condition $s \ll R$ assumed in eq. (3) is therefore fulfilled only for a limitted range of s. For a 120 nm-radius tip, for example, the application of eq. (3) is restricted for $s < 120$ nm. This means that the linear relation between C and $\ln s$ predicted by eq. (3) is actually realized as the reduced slope in the small s region, not at large separations. The change in ΔC around $s \sim 100$ nm is not the deviation from eq. (3) but the transition to the low-s behavior of eq. (3). Figure 3 is an enlarged plot of the $\Delta C - s$ curve for a 120 nm tip. A straight line is a fit to eq. (3) for the part of $\Delta C - s$ curve satisfying the condition $s < R$. From such fittings, we can in turn calculate the tip radius using eq. (4). The tip radii obtained from these data fitting are compared in Table 1 with the values estimated from SEM micrographs. The agreement is excellent. This result demonstrates that the classical spherical tip model is valid for the tip-sample capacitance in the non-tunneling region and that the gap dependence of the capacitance can be described by eq. (3) just before the onset of tunneling. There is no indications of quantum effects.

We note that the spherical tip model is successful only for the low-s part of the ΔC curves of sharp tips. For sharp tips at small separations, a strong field concentration reduces the effective electrode surface to the tip apex which can be well approximated as a hemisphere. This explains the limitted success of the spherical tip model. For treating the high-s behavior of sharp tips and the ΔC curves of dull tips, we have to take into account the entire tip geometry. Theoretical calculations of the capacitance for "truncated cone + hemisphere" tips are now under way. Preliminary result for a sharp tip is found to be in good agreement with the observed $\Delta C - s$ behavior shown in Fig. 3.

5.2. Tunneling region

There are some technical difficulties in capacitance measurements in the tunneling region. The tunneling re-

Table 1
Comparison of two tip radii R and R_{SEM}. R is calculated from the slope of the $\Delta C - s$ curve using eq. (4), and R_{SEM} is obtained from SEM observation.

Sample	R (nm)	R_{SEM} (nm)
1	124	120
2	76	60
3	36	30
4	100	100
5	40	60

sistance effectively shunts the tip-sample capacitor and makes it almost impossible to measure its capacitance with an AC bridge. However, our AC bridge works even for leaky capacitors and gives a conductance together with its capacitance unless the tunneling current exceeds a limitting value. We can therefore extend our measurements into the tunneling region as far as allowed by the operating range of our AC bridge.

Fine control of the gap distance is an another technical problem. During the capacitance measurements, an STM feedback circuit is disconnected from the tip-sample junction and replaced by the AC bridge. Ordinary STM feedback control cannot be used here. Since we can measure the conductance with the AC bridge, a possible way of gap control is to use this conductance, instead of tunneling corrent, as a gap-sensing signal and makes a feedback control with it. This gap-control system is under construction and not available at present. Nevertheless we could obtain some preliminary capacitance data in the tunneling region when the sample approaches to the tip due to thermal drifting.

Figure 4 shows the capacitance measured during the thermal drift. The data are presented as a relative change from a value at large distances and plotted against the conductance. Note that higher conductance corresponds to smaller gap distance. Despite a large scatter in the data, perhaps due to the lack of gap-control, one can see a general trend of decrease in capacitance as the gap distance is reduced. A quite unexpected finding here is that the capacitance drop in Fig. 4 is a few orders of magnitude larger than the ΔCs in Figs. 1-3 (compare the vertical scale in Fig. 4 with those of Figs. 1-3). Such a decrease in ΔC as $s \to 0$ is compatible with none of the gap denpendence discussed in §2 and §3 except eq. (2). The data are, however, too preliminary to make any definite conclusions. More data accumulation, with fine gap control, is thus highly warranted for further understanding of the nature of STM capacitance in the tunneling region.

6. Conclusion

Tip-Sample capacitance in STM has been one of the least studied properties of STM. This is simply because the STM capacitance is irrelevant to STM imaging. Little accumulation of theoretical and experimental data at present unfortunately leads to many inconsistencies and the lack of unified understanding of the STM capacitance. It does not mean that the STM capacitance is not a quantity of marginal importance. On the contrary, as we show in this article, the STM capacitance is closely related to some fundamental problems of capacitance in mesoscopic and atomistic scales and is of much interest in its own light.

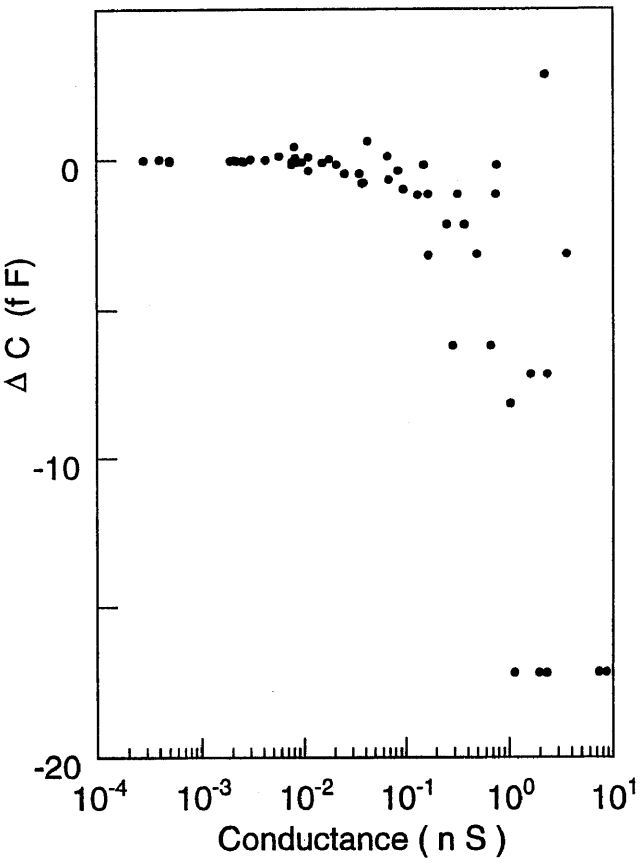

Figure 4. Tip-sample capacitance in the tunneling region is plotted as a function of tunneling conductance. The experimental data show large scatter and a tendency of anomalous decrease at smaller separations.

1) N. D. Lang and W. Kohn: Phys. Rev. **B7** (1973) 3541.
2) M. Büttiker, H. Thomas and A. Prêtre: Phys. Lett. A **180** (1993) 364.
3) M. Büttiker: J. Phys.: Condens. Matter **5** (1993) 9361.
4) T. Christen and M. Büttiker: Phys. Rev. Lett. **77** (1996) 143.
5) V. A. Gopar, P. A. Mello and M. Büttiker: Phys. Rev. Lett. **77** (1996) 3005.
6) J. R. Matey and J. Blanc: J. Appl. Phys. **57** (1985) 1437.
7) C. D. Bugg and P. J. King: J. Phys. E: Sci. Instrum. **21** (1988) 147.
8) C. C. Williams, W. P. Hough and S. A. Rishton: Appl. Phys. Lett. **55** (1989) 203.
9) Y. Akama, A. Sakai, K. Sugihara, N. Shoda, H. Tokumoto, S. Okayama, K. Kajimura and M.

Ono: *Technical Digest of the 8th Sensor Symposium* (Tokyo, 1989) p. 165.
10) H. P. Kleinknecht, J. R. Sandercock and H. Meier: Scanning Microscopy **2** (1988) 1839.
11) R. C. Barret and C. F. Quate: J. Appl. Phys. **70** (1991) 2725.
12) Y. Martin, D. W. Abraham and H. K. Wickramasinghe: Appl. Phys. Lett. **52** (1988) 1103.
13) B. D. Terris, J. E. Stern D. Rugar and H. J. Mamin: Phys. Rev. Lett. **63** (1989) 2669.
14) H. Yokoyama, T. Inoue and J. Itoh: Appl. Phys. Lett. **65** (1994) 3143.
15) P. J. M. van Bentum, H. van Kempen, L. E. C. van de Leemput and P. A. A. Teunissen: Phys. Rev. Lett. **60** (1988) 369.
16) R. Wilkins, E. Ben-Jacob and R. C. Jaklevic: Phys. Rev. Lett. **63** (1989) 801.
17) C. Schönenberger, H. van Houten, J. M. Kerkhof and H. C. Donkersloot: Appl. Surf. Sci. **67** (1993) 222.
18) D. Anselmetti, T. Richmond, A. Baratoff, G. Borer, M. Dreier, M. Bernasconi and H. -J. Güntherodt: Europhys. Lett. **25** (1994) 297.
19) L. Wang, M. E. Taylor and M. E. Welland: Surf. Sci. **322** (1995) 325.
20) C. T. Black, M. T. Tuominen and M. Tinkham: Phys. Rev. **B50** (1994) 7888.
21) R. P. Andres, T. Bein, M. Doroji, S. Feng, J. I. Henderson, C. P. Kubiak, W. Mahoney, R. G. Osifchin and R. Reifenberger: Science **272** (1996) 1323.
22) S. Weiss, D. Botkin, D. F. Ogletree, M. Salmeron and D. S. Chemla: phys. stat. sol. (b) **188** (1995) 343.
23) R. H. M. Groeneveld and H. van Kempen: Appl. Phys. Lett. **69** (1996) 2294.
24) J. P. Kauppinen and J. P. Pekola: Phys. Rev. Lett. **77** (1996) 3889.
25) S. Kurokawa, M. Yuasa, Y. Hasegawa and A. Sakai: Surf. Sci. **357-358** (1996) 532.
26) A. Sakai, S. Kurokawa and Y. Hasegawa: J. Vac. Sci. Technol. **A14** (1996) 1219.